Organic & Biomolecular Chemistry

Accepted Manuscript

This article can be cited before page numbers have been issued, to do this please use: M. L. Agazzi, V. Almovodar, N. S. Gsponer, S. G. Bertolotti, A. Tomé and E. N. Durantini, *Org. Biomol. Chem.*, 2020, DOI: 10.1039/C9OB02487E.

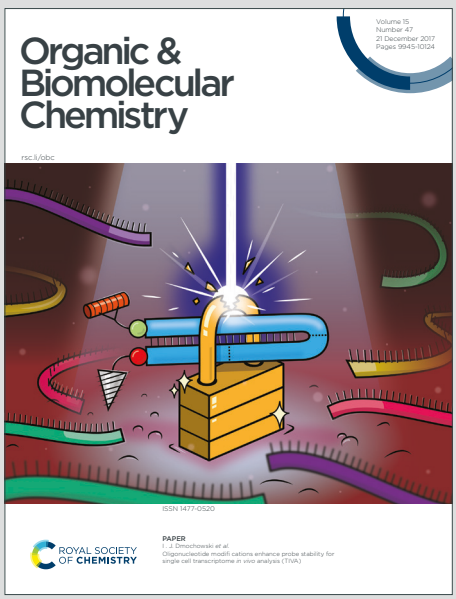

ROYAL SOCIETY OF CHEMISTRY

rsc.li/obc

Diketopyrrolopyrrole–fullerene C_{60} architectures as highly efficient heavy atom-free photosensitizers: synthesis, photophysical properties and photodynamic activity

View Article Online
DOI: 10.1039/C9OB02487E

Maximiliano L. Agazzi[a], Vitor A. S. Almodovar[b], Natalia S. Gsponer[a], Sonia Bertolotti[a], Augusto C. Tomé[b,*], Edgardo N. Durantini[a,*]

[a] *IDAS-CONICET, Departamento de Química, Facultad de Ciencias Exactas, Físico-Químicas y Naturales, Universidad Nacional de Río Cuarto, Ruta Nacional 36 Km 601, X5804BYA Río Cuarto, Córdoba, Argentina.*

[b] *QOPNA & LAQV-REQUIMTE, Department of Chemistry, University of Aveiro, 3810-193, Aveiro, Portugal*

Abstract

Chromophore-fullerene C_{60} hybrids present interesting properties to act as heavy atom-free photosensitizers and reactive oxygen species (ROS) producers. Here, two new diketopyrrolopyrrole–C_{60} conjugates were efficiently synthesized and characterized. Conjugates show broadband absorption in the visible spectral region, in which diketopyrrolopyrrole dyes act as light-harvesting antenna with very high capacity to populate excited triplet states. Furthermore, the ability of diketopyrrolopyrrole–C_{60} systems to generate singlet molecular oxygen was explored for the first time in solvents of different polarities. The experimental results show that these architectures present very high production rates of this ROS. In addition, a preliminary study on *Staphylococcus aureus* cell suspensions indicates that both conjugates induced phototoxicity after irradiation with green LED light. Thus, the data obtained prove evidence that these

* Corresponding authors.

E-mail address: actome@ua.pt (A.C. Tomé), edurantini@exa.unrc.edu.ar (E.N. Durantini)

diketopyrrolopyrrole–C_{60} architectures act as potential heavy atom-free photosensitizers in photodynamic inactivation of microorganisms and other singlet oxygen-mediated applications.

View Article Online
DOI: 10.1039/C9OB02487E

Keywords: fullerene, diketopyrrolopyrrole, heavy atom-free photosensitizer, ROS, photodynamic inactivation.

Introduction

Triplet photosensitizers (PSs) are compounds that produce efficiently the triplet excited state upon photoexcitation.[1] These PSs have been studied in a wide range of applications, namely in photocatalytic organic reactions,[2,3] photovoltaics,[4,5] triplet–triplet annihilation upconversion,[6,7] and photodynamic therapy.[8,9] In the last two decades, also were explored as antimicrobial agents for the photodynamic inactivation of drug-resistant microbes.[10–13] For phototherapeutic application, an appropriate PS should show strong absorption of visible light, effective intersystem crossing (ISC) to form excited triplet states with a long triplet lifetime and high production of reactive oxygen species (ROS).[14–16]

Until today, a large number of molecules, as phenothiazines and porphyrins, have been developed and studied as phototherapeutic agents.[13,17–21] Different chromophores have been converted into PSs by incorporation of heavy atoms that increase the ISC and consequently the production of excited triplet state. In this sense, transition metal complexes and chromophores bearing bromine or iodine atoms have been designed and tested.[9,22–26] Nevertheless, the heavy atom effect is not always efficient, especially in large molecules. In addition, the synthesis of the transition metal complexes is usually not very cost-effective, and brominated or iodinated compounds can present high toxicity in the dark.[27,28]

Within this context, the design of heavy atom-free PSs emerged as an exciting challenge.[29,30] However, the efficiency of the ISC mechanism is difficult to predict in organic chromophores without heavy atoms. A powerful approach to generate heavy atom-free PSs with efficient and

View Article Online
DOI: 10.1039/C9OB02487E

predictable ISC is to attach an intramolecular spin converter to the fluorophores. In this way, fullerene C_{60} is a particularly interesting spin converter,[1,31] since it exhibits a highly efficient ISC inherent with a near unity yield.[32] Thus, C_{60} derivatives have been evaluated as phototherapeutic agents.[33–36] However, pristine C_{60} is not an ideal PS because its absorptions bands in the visible are very weak.[32,37] Several examples of donor–acceptor systems formed by a chromophore (as light-harvesting antenna and intramolecular energy donor) and fullerene C_{60} (as intramolecular energy acceptor) have been reported.[1] Upon photoexcitation of the light-harvesting moiety, these conjugates can generate excited triplet states by energy transfer (EnT).[38–40] In addition, since the C_{60} moiety is a good electron acceptor, these donor–acceptor systems frequently present ability to generate photoinduced electron transfer (PeT) processes, forming charge-separated states.[41,42] In various reports, it was found that the exited triplet states of light-harvesting antenna can be populated efficiently by charge recombination process.[43–49]

A significant number of C_{60}–chromophore conjugates were reported and evaluated as triplet PSs. Among others, as chromophores have been used 4,4-difluoro-4-bora-3*a*,4*a*-diaza-*s*-indacene (BODIPY),[50–55] porphyrins,[56–59] fluorenes,[60–62] perylenebisimides,[63,64] naphthalenediimides,[65] fluorescein,[66] and rhodamine derivatives.[67,68] Recently, chromophores based on diketopyrrolopyrrole (DPP) derivatives have attracted interest, and have been explored in different applications, due to their high absorption coefficients, high fluorescence quantum yields, excellent photostability and considerable synthetic versatility.[69–71] In the last decade, DPP derivatives have been studied as PSs for photodynamic therapy (PDT).[72–74] However, because DPPs alone have a very poor ISC, different strategies were developed to mimic the heavy atom effect.[75–77]

In this context, DPP dyes could act as light-harvesting antenna in donor-C_{60} systems to generate efficient heavy atom-free triplet PSs. In 2010, Janssen and co-workers reported the synthesis of **C_{60}-DPP-C_{60}** structures and studied their optical and electrochemical properties, aiming their potential application in organic photovoltaics.[78,79] Nevertheless, to the best of our knowledge, the use of DPP-C_{60} systems for singlet molecular oxygen, $O_2(^1\Delta_g)$, production has not

View Article Online
DOI: 10.1039/C9OB02487E

yet been explored. Here, two new donor–acceptor systems (**DPP-C_{60}** and **C_{60}-DPP-C_{60}**) based on the covalent binding of DPP and *N*-methylfulleropyrrolidine units were rationally designed and synthesized. Their spectroscopic and photodynamic properties were studied in solvents of different polarities and compared with those of DPPs and C_{60} reference compounds. Triplet generation was explored with transient absorption measurements and $O_2(^1\Delta_g)$ production was evaluated by the photooxidation reaction of dimethylanthracene (DMA). Photodynamic action was also explored *in vitro* for the inactivation of *S. aureus* cells. The results obtained indicate that C_{60}–diketopyrrolopyrrole architectures have interesting properties to act as potential heavy atom-free PSs in phototherapies and related applications.

Experimental

General

NMR spectra were obtained using on a Bruker DRX 300 Advance operating at 300.13 MHz (for ^{1}HNMR spectra) or at 75.47 MHz (for ^{13}C NMR spectra). Micromass Q-TOF-2™ (Bruker Daltonics, MA, USA) and MALDI-TOF-MS spectrometers were used to obtain the mass spectra. Absorption and fluorescence spectra were carried out in a Shimadzu UV-2401PC spectrometer (Shimadzu Corporation, Tokyo, Japan) or a Spex FluoroMax spectrofluorometer (Horiba Jobin Yvon Inc, Edison, NJ, USA), respectively. Fluence rates were determined with a Radiometer Laser Mate-Q (Coherent, Santa Clara, CA, USA). Experiments of photooxidation of substrate were carried out with a Cole-Parmer illuminator 41720-series (Cole-Parmer, Vernon Hills, IL, USA) with a 150 W halogen lamp through a high intensity grating monochromator (Photon Technology Instrument, Birmingham, NJ, USA) with a fluence rate of 0.75 mW/cm^2 at 515 nm. The light source to irradiate microbial cells was a light-emitting diode (LED) array that emitted green light at a center wavelength of 510 nm with a fluence rate of 5 mWcm^2. The solvents used in the chemical transformations were mostly of analytical purity. Commercial solvents used in the purification processes were previously distilled. The progress of reactions was monitored by TLC performed on

View Article Online
DOI: 10.1039/C9OB02487E

silica gel 60 (Merck, Darmstadt, Germany) coated plastic sheets. Silica gel 60 (Merck) with particle size 0.063-0.200 mm was used for column separations. Purifications by preparative TLC were performed on glass plates (20 x 20 cm) precoated with a layer of silica gel 60 (Merck) with a thickness of 0.5 mm and activated in the oven at 100 °C for 12 h.

Synthesis

5,10,15,20-Tetrakis(4-methoxyphenyl)porphyrin (**TMP**) and 3,6-bis(4-chlorophenyl)-2,5-dihydropyrrolo[3,4-*c*]pyrrole-1,4-dione (**DPP0**) were purchased from Sigma-Aldrich (Milwaukee, WI, USA). 1,3,5,7-Tetramethyl-8-[4-(dimethylaminophenyl]-4,4-difluoro-4-bora-3*a*,4*a*-diaza-*s*-indacene (**BDP**) and *N*-methylfulleropyrrolidine (**MC_{60}**) were synthesized using the general synthetic methods previously reported.[80,81]

3,6-Bis(4-chlorophenyl)-2,5-dipentyl-2,5-dihydropyrrolo[3,4-*c*]pyrrole-1,4-dione (DPP1). A suspension of **DPP0** (500 mg, 1.40 mmol) and K_2CO_3 (966 mg, 7 mmol) in *N*,*N*-dimethylformamide (DMF) (60 mL) was heated at 65 ºC under nitrogen atmosphere during 30 min. At this temperature, and under vigorous stirring, a solution of 1-iodopentane (1.40 g, 0.883 mL, 7 mmol) in DMF (8 mL) was added dropwise. The mixture was stirred for 24 h at 120 °C. After cooling to room temperature, the mixture was diluted with CH_2Cl_2 and water. The organic layer was separated and washed with water and brine. The product was isolated by column chromatography on silica gel using CH_2Cl_2 as the eluent. Crystallization from methanol afforded the pure compound **DPP1** as bright red crystals (270 mg, 39% yield). M.p. = 205.8-206.8 ºC; ^{1}HNMR (300 MHz, $CDCl_3$) δ (ppm): 0.83 (t, J = 6.8 Hz, 6H), 1.18–1.28 (m, 8H), 1.51–1.59 (m, 4H), 3.73 (t, J = 7.7 Hz, 4H), 7.47–7.51 (m, 4H), 7.72–7.77 (m, 4H); ^{13}C NMR (75 MHz, $CDCl_3$) δ (ppm) 13.89, 22.13, 28.82, 29.13, 41.87, 109.90, 126.50, 129.28, 129.98, 137.35, 147.38, 162.47; MS (ESI): *m/z* 497.3 $(M+H)^+$

View Article Online
DOI: 10.1039/C9OB02487E

3-(4-Chlorophenyl)-2,5-dipentyl-6-[4-(4,4,5,5-tetramethyl-1,3,2-dioxaborolan-2-yl)phenyl]-2,5-dihydropyrrolo[3,4-*c*]pyrrole-1,4-dione (DPP2) and 2,5-dipentyl-3,6-bis[4-(4,4,5,5-tetramethyl-1,3,2-dioxaborolan-2-yl)phenyl]-2,5-dihydropyrrolo[3,4-*c*]pyrrole-1,4-dione (DPP3). A mixture of **DPP1** (150 mg, 0.30 mmol), bis(pinacolato)diboron (900 mg, 3.6 mmol), KOAc (206 mg, 2.1 mmol), $Pd_2(dba)_3$ (11.9 mg, 0.013 mmol), and XPhos (3 mg, 0.008 mmol) in 1,4-dioxane (8.0 mL) was stirred under nitrogen at 110 °C for 4 h. After cooling to room temperature, the mixture was diluted with CH_2Cl_2. Water was added, the organic layer was separated and then washed again with brine and water. The solvent was removed under reduced pressure and the resulting yellow solid (a mixture of compounds **DPP2** and **DPP3**) was used directly in the next step without further purification.

4'-{4-(4-Chlorophenyl)-3,6-dioxo-2,5-dipentyl-2,3,5,6-tetrahydropyrrolo[3,4-c]pyrrol-1-yl}-[1,1'-biphenyl]-4-carbaldehyde (DPP4) and 4',4'''-3,6-dioxo-2,5-dipentyl-2,3,5,6-tetrahydropyrrolo[3,4-*c*]pyrrole-1,4-diyl)bis([1,1'-biphenyl]-4-carbaldehyde) (DPP5). The solid obtained in the previous step (a mixture of **DPP2** and **DPP3**), 4-iodobenzaldehyde (94 mg, 0.404 mmol), $Pd(PPh_3)_4$ (29 mg, 0.025 mmol), Cs_2CO_3 (132 mg, 0.404 mmol) were dissolved in toluene/DMF (2:1) (45 mL) and the solution was stirred for 4 h at 80 °C under a nitrogen atmosphere. After cooling to room temperature, the mixture was diluted with CH_2Cl_2. Water was added, the organic layer was separated and then washed again with brine and water. The two aldehydes were separated by column chromatography on silica gel using CH_2Cl_2 as the eluent. **DPP4** (red solid, 66 mg, 35% yield) was eluted first, followed by **DPP5** (purple solid, 72 mg, 42% yield). **DPP4**. M.p. = 142.3-143.2 ºC; ^{1}H NMR (300 Hz, $CDCl_3$) δ (ppm): 0.84 (t, J = 6.7 Hz, 6H, F-H), 1.24–1.29 (m, 8H, E and E‘-H), 1.60–1.69 (m, 4H, DH), 3.72–3.82 (m, 4H, C-H), 7.49–7.55 (m, 2H, A-H) 7.76–7.84 (m, 6H, D-H), 7.92–8.02 (m, 4H, A-H), 10.09 (s, 1H, E-H); ^{13}C NMR (75 MHz, $CDCl_3$) δ (ppm): 13.92, 13.94, 22.16, 22.18, 28.86, 28.89, 29.90, 29.24, 41.98, 42.09, 110.10, 126.58, 127.78, 127.86, 128.11, 129.34, 129.38, 130.0, 130.44, 135.75, 137.35, 142.31, 145.79,

View Article Online
DOI: 10.1039/C9OB02487E

147.28, 148.01, 162.61, 162.64, 191.83; MS (ESI): *m/z* 567.4 $(M+H)^+$. **DPP5**. M.p. = 177.4-179.2 ºC; ^{1}H NMR (300 Hz, $CDCl_3$) δ (ppm), 0.83 (t, *J* = 6.7 Hz, 6H), 1.22–1.28 (m, 8H), 1.62–1.70 (m, 4H), 3.81 (t, *J* = 7.6 Hz, 4H), 7.79–7.83 (m, 8H), 7.94–8.01 (m, 8H), 10.08 (s, 2H); ^{13}C NMR (75 MHz, $CDCl_3$) δ (ppm) 13.94, 22.19, 28.91, 29.27, 42.13, 110.24, 127.79, 127.87, 128.16, 129.4, 130.45, 135.75, 142.30, 145.80, 147.91, 162.75, 191.84; MS (ESI): *m/z* 637.4 $(M+H)^+$.

DPP-C_{60}. A solution of **DPP4** (50 mg, 0.07 mmol), C_{60} (50 mg, 0.07 mmol), and *N*-methylglycine (7 mg, 0.07 mmol) in anhydrous toluene (60 mL), under argon atmosphere, was stirred at reflux for 6 h. The solvent was removed under reduced pressure and the product was purified by flash chromatography (silica gel, toluene/cyclohexane from 80:20 to 100:0). Pure **DPP-C_{60}** (31 mg; 40% yield) was obtained. M.p. > 250 °C; ^{1}HNMR ($CDCl_3$, TMS) δ (ppm) 0.83 (t, 6H, CH_3, *J* = 6.5 Hz), 1.31 (broad, 8H, CH_2), 1.60 (broad, 4H, CH_2), 2.86 (s, 3H, N-CH_3), 3.70-3.80 (m, 4H, $CH_2(CH_2)_3CH_3$), 4.30 (d, 1H, pyrrolidine ring, *J* = 9 Hz), 5.02 (d, 2H, pyrrolidine ring, *J* = 9 Hz) 7.35 (d, 2H, Ar-H, *J* = 6 Hz), 7.51 (d, 2H, Ar-H, *J* = 9 Hz), 7.79 (m, 6H, Ar-H), 7.90 (d, 2H, Ar-H, *J* = 9 Hz); ^{13}C NMR (126 MHz, $CDCl_3$) δ (ppm) 162.73, 162.55, 156.22, 154.02, 153.34, 153.22, 148.52, 147.33, 147.08, 146.83, 146.73, 146.47, 146.33, 146.31, 146.24, 146.20, 146.16, 146.13, 145.96, 145.78, 145.57, 145.47, 145.37, 145.35, 145.30, 145.25, 145.19, 144.73, 144.59, 144.43, 144.39, 143.25, 143.17, 143.02, 142.72, 142.60, 142.57, 142.29, 142.27, 142.18, 142.16, 142.12, 142.09, 142.07, 142.00, 141.96, 141.86, 141.72, 141.57, 140.22, 140.20, 139.94, 139.80, 139.57, 138.53, 138.45, 137.19, 137.15, 136.93, 136.53, 135.94, 135.74, 129.98, 129.29, 129.25, 127.45, 127.33, 127.05, 126.67, 124.47, 124.00, 119.10, 110.14, 109.78, 83.31, 70.08, 69.12, 42.11, 41.93, 40.13, 34.88, 34.54, 31.95, 31.52, 31.45, 30.20, 29.68, 29.39, 29.22, 28.90, 28.86, 22.72, 22.19, 22.16, 14.15, 13.95, 13.93; MS (MALDI-TOF) *m/z*: 1314.30 $(M+H)^+$; 1313.28 calculated for $C_{97}H_{40}ClN_3O_2$.

DOI: 10.1039/C9OB02487E

C_{60}-DPP-C_{60}. A solution of **DPP5** (50 mg, 0.06 mmol), C_{60} (130 mg, 0.18 mmol), and *N*-methylglycine (13.36 mg, 0.15 mmol) in anhydrous toluene (60 mL), under argon atmosphere, was stirred at reflux for 12 h. The solvent was removed under reduced pressure and the product was purified by flash chromatography (silica gel, toluene/cyclohexane from 80:20 to 100:0) Pure C_{60}-DDP-C_{60} (46 mg; 36% yield) was obtained. M.p. > 250 °C; ^{1}HNMR ($CDCl_3$, TMS) δ (ppm) 0.83 (t, 6H, CH_3, J = 6.5 Hz), 1.31-1.40 (m, 8H, CH_2), 1.61 (broad, 4H, CH_2), 2.85 (s, 6H, N-CH_3), 3.75 (t, 4H, $CH_2(CH_2)_3CH_3$)), 5.25 (m, 4H, pyrrolidine ring), 4.97-5.03 (m, 2H, pyrrolidine ring), 7.65-7.80 (m, 8H, Ar-H), 7.85-7.95 (m, 8H, Ar-H); ^{13}C NMR (126 MHz, $CDCl_3$) δ (ppm) 161.83, 156.17, 153.93, 153.32, 147.76, 147.71, 147.38, 146.69, 146.30, 146.05, 145.86, 145.40, 144.49, 143.27, 142.70, 142.26, 140.37, 138.90, 138.21, 138.14, 137.54, 137.11, 135.86, 134.94, 130.21, 129.65, 129.60, 129.14, 128.66, 128.41, 127.59, 126.93, 125.52, 125.40, 124.44, 124.09, 119.27, 114.52, 109.79, 83.42, 70.22, 69.09, 41.35, 40.24, 39.22, 37.52, 37.08, 34.76, 34.36, 34.09, 33.62, 33.17, 32.46, 31.60, 30.70, 30.59, 30.47, 30.22, 30.09, 29.94, 29.83, 29.71, 29.51, 29.42, 29.22, 29.14, 28.46, 27.61, 27.22, 26.75, 26.46, 23.75, 23.41, 23.06, 22.79, 21.84, 20.13, 19.64, 14.72, 14.48, 14.43, 12.00, 11.43; MS (MALDI-TOF) *m/z:* 1410.07 $(M\text{-}C_{60})^+$; 1411.32 $(M\text{-}C_{60}+H)^+$; 1410.39 calculated for $C_{106}H_{50}N_4O_2$.

Spectroscopic studies

UV-visible absorption and fluorescence spectra were recorded in a quartz cell of 1 cm path length at 25.0 ± 0.5 °C. The steady-state fluorescence emission spectra were performed exciting the samples at λ_{exc} = 480 nm. Absorbances (<0.05) were matched at the excitation wavelength and the areas of the emission bands were integrated in the range of 490-700 nm. The fluorescence quantum yield (Φ_F) were determined using **BDP** as a reference in acetonitrile.[80] The values of the refractive indices for each of the solvents were considered to calculate the Φ_F in different media.

Transient absorption measurements

View Article Online
DOI: 10.1039/C9OB02487E

The transient absorption spectra were determined in Ar-saturated solutions of toluene and DMF by laser flash photolysis. A 532 nm Nd:YAG (Spectron) laser output was employed as the excitation source. The experiments were performed as previously described.[82] The laser beam was defocused in order to cover all the path length (10 mm) of the analyzing beam from a 150 W Xe lamp. The detection system comprised a PTI monochromator coupled to a Hamamatsu R666 PM photomultiplier. The signals were acquired and averaged by a digital oscilloscope (Hewlett-Packard 54504) and then transferred to a computer.

Photooxidation of 9,10-dimethylanthracene (DMA)

Solutions of DMA (20 μM) and PS in toluene and DMF were irradiated in 1 cm path length quartz cells (2 mL) with monochromatic light at λ_{irr} = 515 nm (PS absorbance 0.1). The kinetics of DMA photooxidation were studied following the decrease of the absorbance (A) at λ_{max} = 378 nm. The observed rate constants (k_{obs}) were obtained by a linear least-squares fit of the semilogarithmic plot of Ln A_0/A *vs*. time. Values of quantum yields of $O_2(^1\Delta_g)$ production (Φ_Δ) were calculated comparing the k_{obs} for the corresponding PS with that for **TMP**, which was used as a reference (Φ_Δ^{DMF} = 0.65 and $\Phi_\Delta^{Toluene}$ = 0.67).[83] Measurements of the sample and reference under the same conditions afforded Φ_Δ for PSs by direct comparison of the slopes in the linear region of the plots. DMA photooxidation by **DPP-C_{60}**, **C_{60}-DPP-C_{60}** and **MC_{60}** was evaluated under irradiation with monochromatic light (λ_{irr} = 515 nm) and visible light. In the last case DMA was evaluated only as a control experiment.

Bacteria and growth conditions

S. aureus ATCC 25923 cells were aerobically cultured under sterile conditions overnight at 37 ºC in 4 mL tryptic soy broth (Britania, Buenos Aires, Argentina).[35] An aliquot (40 μL) of the bacterial culture was aseptically transferred to fresh tryptic soy broth (4 mL) and incubated at 37 ºC to exponential phase of growth (absorbance 0.6 at 660 nm). The cultures were centrifuged (3000

View Article Online
DOI: 10.1039/C9OB02487E

rpm for 15 min) and then, cells were re-suspended in 10 mM phosphate-buffered saline (4 mL) (PBS, pH = 7.2) solution, corresponding to ~10^8 colony forming units (CFU)/mL.

Photosensitized inactivation of bacteria

S. aureus suspensions (2 mL, ~10^8 CFU/mL) in PBS were incubated with 10 μM PS for 15 min in the dark at 37 °C in Pyrex culture tubes (13x100 mm). PS was added from a 0.5 mM stock solution in DMF. Then, 200 μL of each cell suspension were transferred to 96-well microtiter plates (Deltalab, Barcelona, Spain). Cell suspensions were immediately irradiated with green light for 15 min (*S. aureus*). After irradiation, bacterial cells were serially diluted 10-fold in PBS. Cell suspensions were quantified by the spread plate method in triplicate. Viable bacteria were examined and the number of CFU was counted on TS agar plates after ~24 h incubation at 37 ºC in the dark. Control experiments and statistical analysis with microbial cells were carried out as previously indicated.[35]

Results and discussion

Design and synthesis of conjugates DPP-C_{60} and C_{60}-DDP-C_{60}

The synthetic procedures to obtain compounds **DPP-C_{60}** and **C_{60}-DPP-C_{60}** are summarized in Scheme 1 and 2. First, we synthetized two visible light-harvesting antennas based in DPP dyes. Because **DPP0** is almost insoluble in most solvents, the dipentyl substituted **DPP1** was generated by alkylation with 1-iodopentane (step a, Scheme 1). Then, from the reaction of **DPP1** with bis(pinacolato)diboron a mixture of **DPP2** and **DPP3** was obtained (step b, Scheme 1). This mixture was reacted with 4-iodobenzaldehyde (step c, Scheme 1) through a Suzuki coupling to produce the light-harvesting antennas with one or two formyl groups. The two products were separated by flash chromatography and **DPP4** and **DPP5** were isolated in 40% and 36% yield, respectively. Finally, diketopyrrolopyrrole-linked fullerene C_{60} were synthetized by 1,3-dipolar cycloadditions involving *in situ* generated azomethine ylides (Prato reaction) [84]. For these propose, **DPP4** and **DPP5** were reacted with *N*-methylglycine and fullerene C_{60} in refluxing toluene (Scheme 2). Purification by

View Article Online
DOI: 10.1039/C9OB02487E

flash chromatography using toluene/cyclohexane afforded the expected conjugates **DPP-C_{60}** (35% yield) and **C_{60}-DPP-C_{60}** (46% yield).

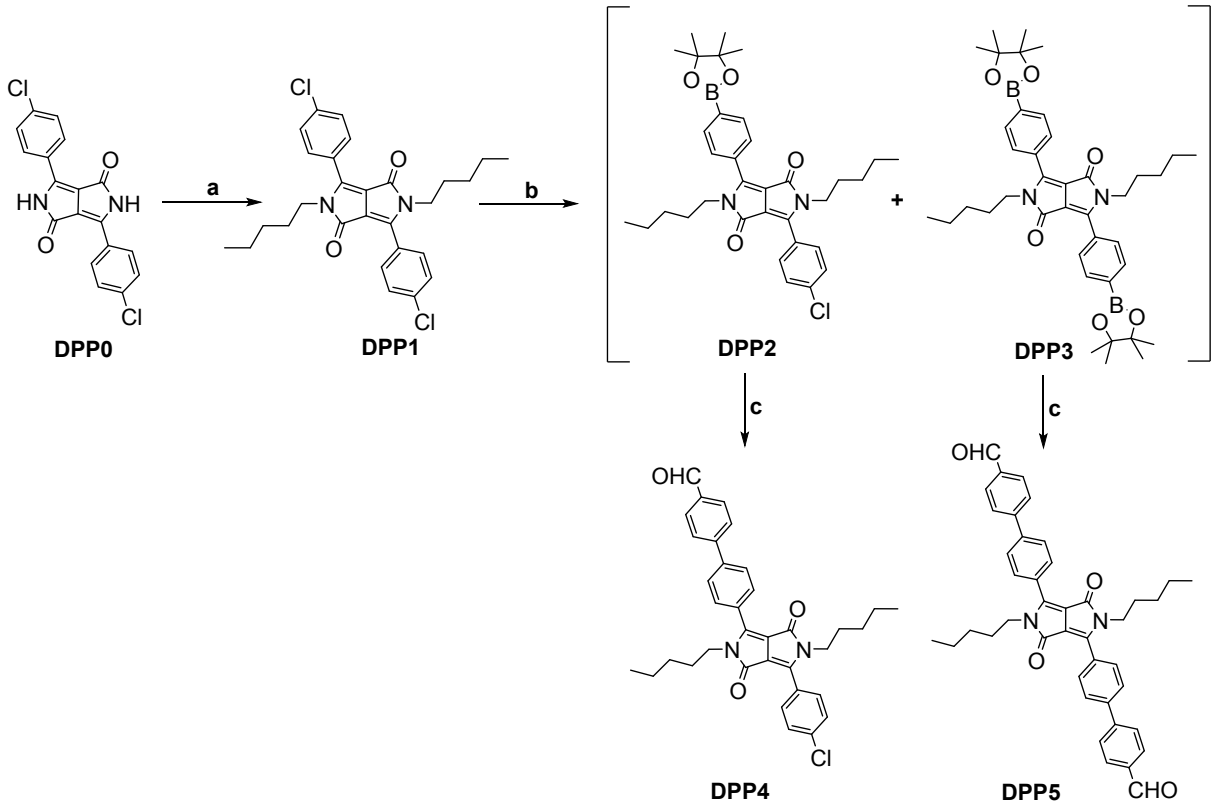

Scheme 1. Synthesis of **DPP4** and **DPP5**. Reagents and conditions: (a) 1-iodopentane, K_2CO_3, DMF, 120 °C, 24 h; (b) bis(pinacolato)diboron, $Pd_2(dba)_3$, XPhos, KOAc, 1,4-dioxane, 110 °C, 4 h; (c) $Pd(PPh_3)_4$, 4-iodobenzaldehyde, Cs_2CO_3, toluene/DMF (2:1), 80 ºC, 4 h.

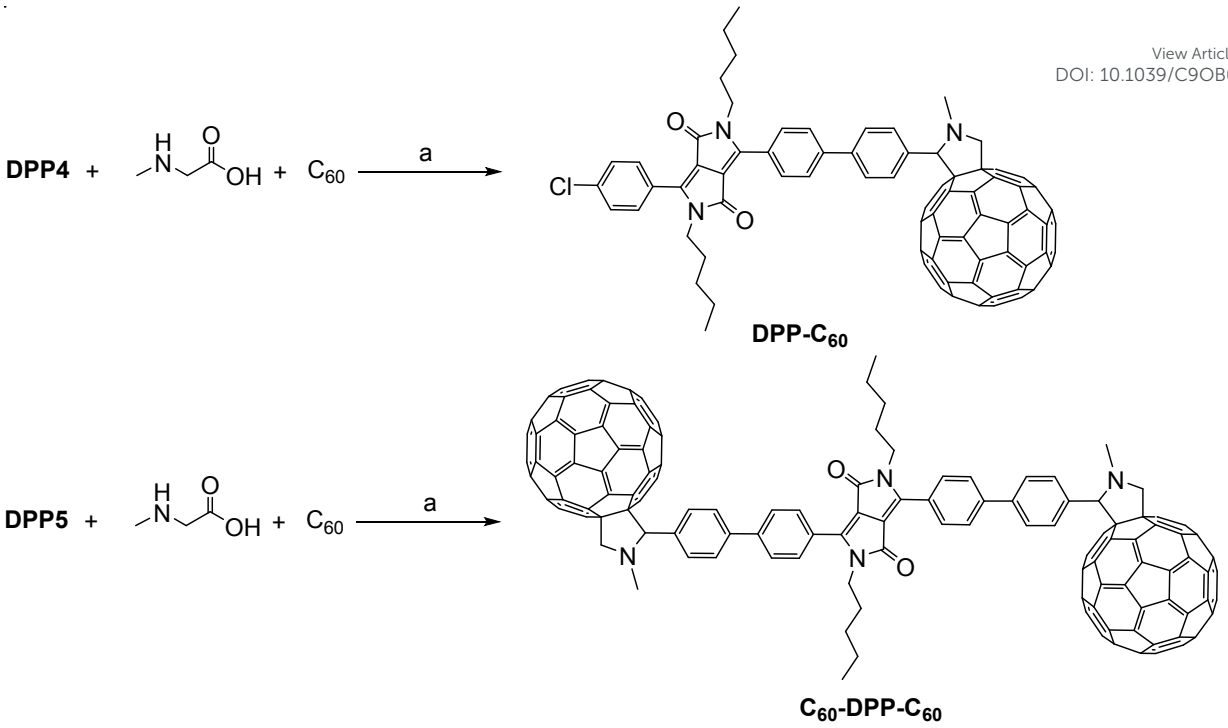

Scheme 2. Synthesis of conjugates **DPP-C_{60}** and **C_{60}-DPP-C_{60}**. Reagents and conditions: (a) toluene, reflux, Ar, 12 h.

Absorption and fluorescence spectroscopic properties

The absorption spectra of **DPP-C_{60}** and **C_{60}-DPP-C_{60}** together with the spectra corresponding to the fullerene (**MC_{60}**, Scheme S1) and DPP moieties (**DPP4** and **DPP5**) are presented in Figure 1. Their spectroscopic characteristics are summarized in Table 1. Both conjugates present a broad band from 400 to 550 nm centered in the green region, corresponding to the absorption of the DPP moiety. Moreover, structures show a peak around 430 nm typical of the *N*-methylfulleropyrrolidine moiety.[81] The absorption in the UV region is very intense because both C_{60} and DPP have high absorptions in that spectral zone. The spectra of conjugates were essentially a linear combination of the spectra of the corresponding moieties. This behavior reveals that the fractions interact weakly in the ground state, retaining each fraction their individual identities. Dyad **DPP-C_{60}** presents the maximum absorption in the visible at 485 nm, showing a small hypsocromomic shift of 5 nm with respect to **DPP4** (Figure 1A). In addition, it shows similar spectroscopic characteristics in solvents of different polarity (Figure S1A). In the case of **C_{60}-DPP-**

View Article Online
DOI: 10.1039/C9OB02487E

C_{60}, the maximum absorption was located at 502 nm, with a very small bathochromic shift (~2 nm) compared to **DPP5** (Figure 1B). Unlike **DPP-C_{60}**, compound **C_{60}-DPP-C_{60}** shows a high aggregation tendency in several solvents (Figure S1B). This behavior is probably due to the presence of two C_{60} units that reduce strongly the solubility of the conjugate in different media.

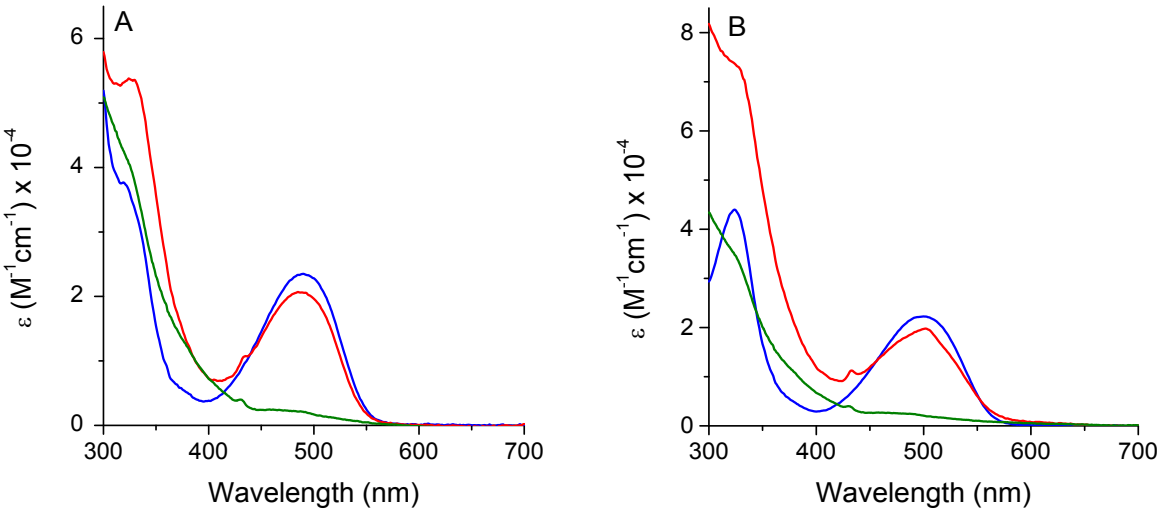

Figure 1. (A) Absorption spectra of **DPP-C_{60}** (red line), **MC_{60}** (green line) and **DPP4** (blue line) and (B) absorption spectra of **C_{60}-DPP-C_{60}** (red line), **MC_{60}** (green line) and **DPP5** (blue line) in toluene.

Fluorescence emission spectra of conjugates and DPPs were registered in toluene and DMF (Figure 2). The samples were excited at 480 nm, where the absorption is mainly due to the DPP fraction. The emission properties of each structure are reported in Table 1. **DPP4** and **DPP5** present signals in toluene and DMF around 560 and 575 nm, respectively. As is well known, these dyes have very high fluorescence emission yields (Table 1).[70] Dyad **DPP-C_{60}** showed only very weak emission in toluene (Φ_F ~ 0.03) and DMF (Φ_F ~ 0.04). The quenching efficiencies were estimated to be $\eta_q \geq 0.95$ and 0.93 in toluene and DMF, respectively. In the case of **C_{60}-DPP-C_{60}**, it showed a very weak emission in toluene (Φ_F ~ 0.06) and quenching efficiencies of 0.93. However, in DMF it presented a surprisingly high emission yield (Φ_F ~ 0.26) with a lower quenching efficiency (η_q =

0.70). In general, the fluorescence studies indicate that the covalent binding of C_{60} produces a relevant quenching of the excited singlet state of the DPPs. This process can be caused by EnT from the singlet excited state of antennas to the C_{60} or by PeT with formation of a charge-separated state.

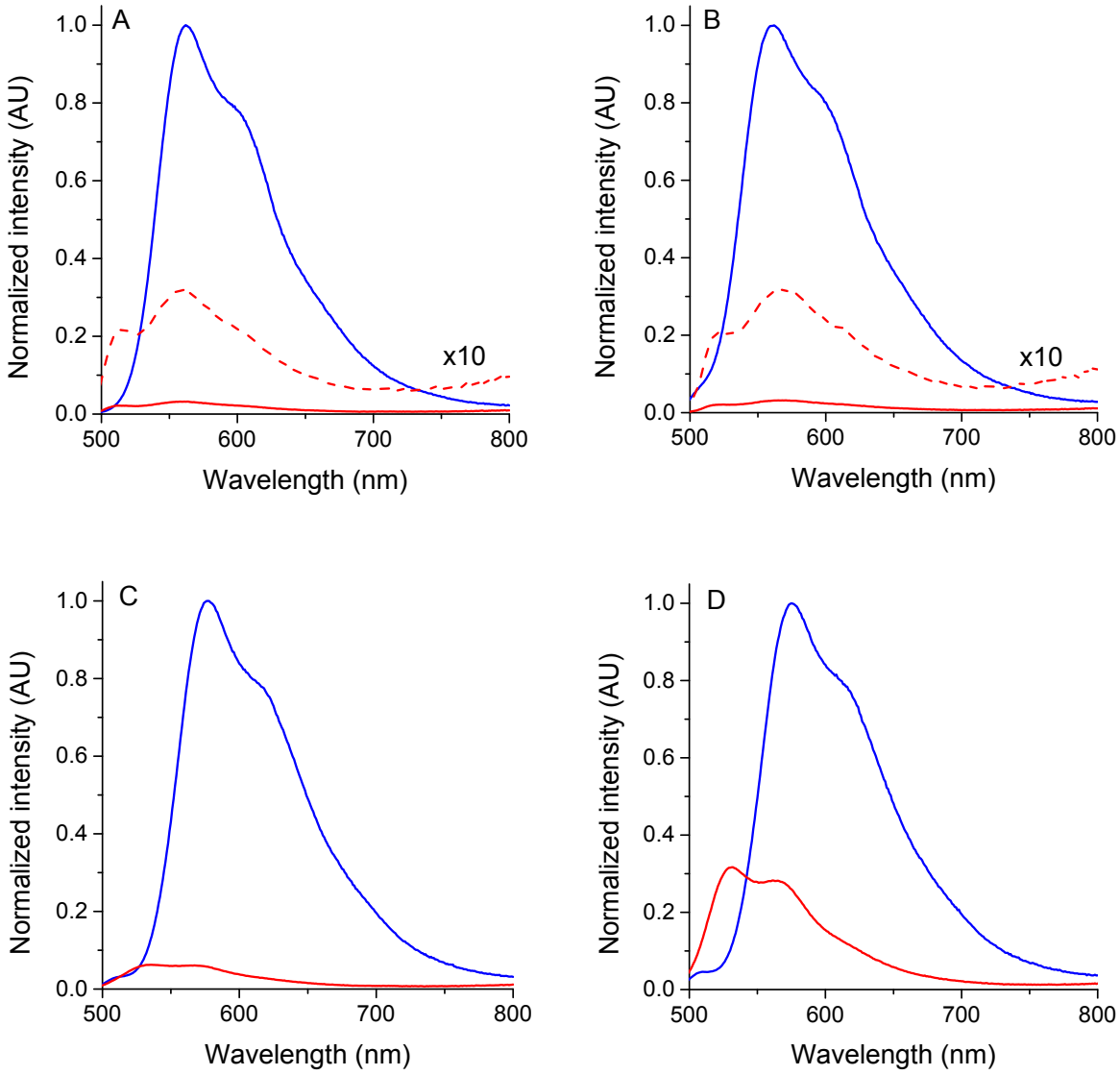

Figure 2. Fluorescence emission spectra of **DPP-C_{60}** (red line) and **DPP4** (blue line) in (A) toluene and (B) DMF and of **C_{60}-DPP-C_{60}** (red line) and **DPP5** (blue line) in (C) toluene and (D) DMF.

Table 1. Spectroscopic parameters and fluorescence quantum yields (Φ_F) of DPP derivatives.

Parameters	Media	**DPP4**	**DPP5**	**DPP-C_{60}**	**C_{60}-DPP-C_{60}**

View Article Online
DOI: 10.1039/C9OB02487E

λ_{max}^{Abs} (nm)	toluene	490	500	485	502
λ_{max}^{Abs} (nm)	DMF	481	492	481	481
ε ($M^{-1}cm^{-1}$)	toluene	23.510	22.265	20.700	19.800
λ_{max}^{Em} (nm)	toluene	562	577	564	535/567
Φ_F	toluene	0.72±0.02	0.92±0.03	0.03±0.01	0.06±0.01
λ_{max}^{Em} (nm)	DMF	562	575	568	532/561
Φ_F	DMF	0.87±0.03	0.87±0.03	0.04±0.01	0.26±0.02

Φ_F were calculated with **BDP** in acetonitrile (Φ_Δ = 0.71) as reference.

Transient absorption spectra

In order to evaluate the efficiency of the conjugates to produce excited triplet states, transient absorption measurements were performed using laser flash photolysis. For this proposal, the fraction of DPP in each conjugate was selectively excited upon pulsed laser at 532 nm. Transient spectra of **DPP4** and **DPP5** in toluene were also recorded under the same experimental conditions (Figures S2 and S3). As expected, both structures present a very poor production of triplet excited states.[75,78] Figure 3 shows the transient spectra obtained for **DPP-C_{60}** in toluene and DMF. In toluene, transient absorption spectra showed the appearance of two positive peaks centered at 390 and 540 nm (Figure 3A). Furthermore, bleaching of small intensity bands at 320 and 470 nm was observed, which coincides with the steady-state absorption of **DPP4** (Figure 1A). The transient bands can be assigned to the absorption of the excited triplet state of the DPP moiety (^{3}DPP*). This assignment was confirmed by recording the transient spectrum of **DPP4** (Figure S2). Interestingly, the intensity of the positive transient signal for the **DPP-C_{60}** was 20 times greater in relation to that obtained for **DPP4**. The decays at the maximum transient wavelengths were adjusted by a second-order exponential, obtaining two triplet-state lifetimes of 73 μs and 17 μs, indicating that two transient species are present. Whereas the **DPP4** lifetime is 40 μs (Figure S2B), the longest lifetime

can be assigned to the ^{3}DPP*. On the other hand, the shortest life time may correspond to the triplet of C_{60} ($^3C_{60}^*$).[39] It is well known that fullerene C_{60} has transient bands around 700 nm.[43] **DPP-C_{60}** spectra present absorptions with small intensities in this region, which would indicate that the $^3C_{60}^*$ is populated but in a much smaller magnitude in relation to the ^{3}DPP*. In DMF, similar spectroscopic characteristics were observed (Figure 3C and 3D). The absorption of the triplets was lower than in toluene, possibly due to a partial aggregation of the dyad in the more polar solvent.

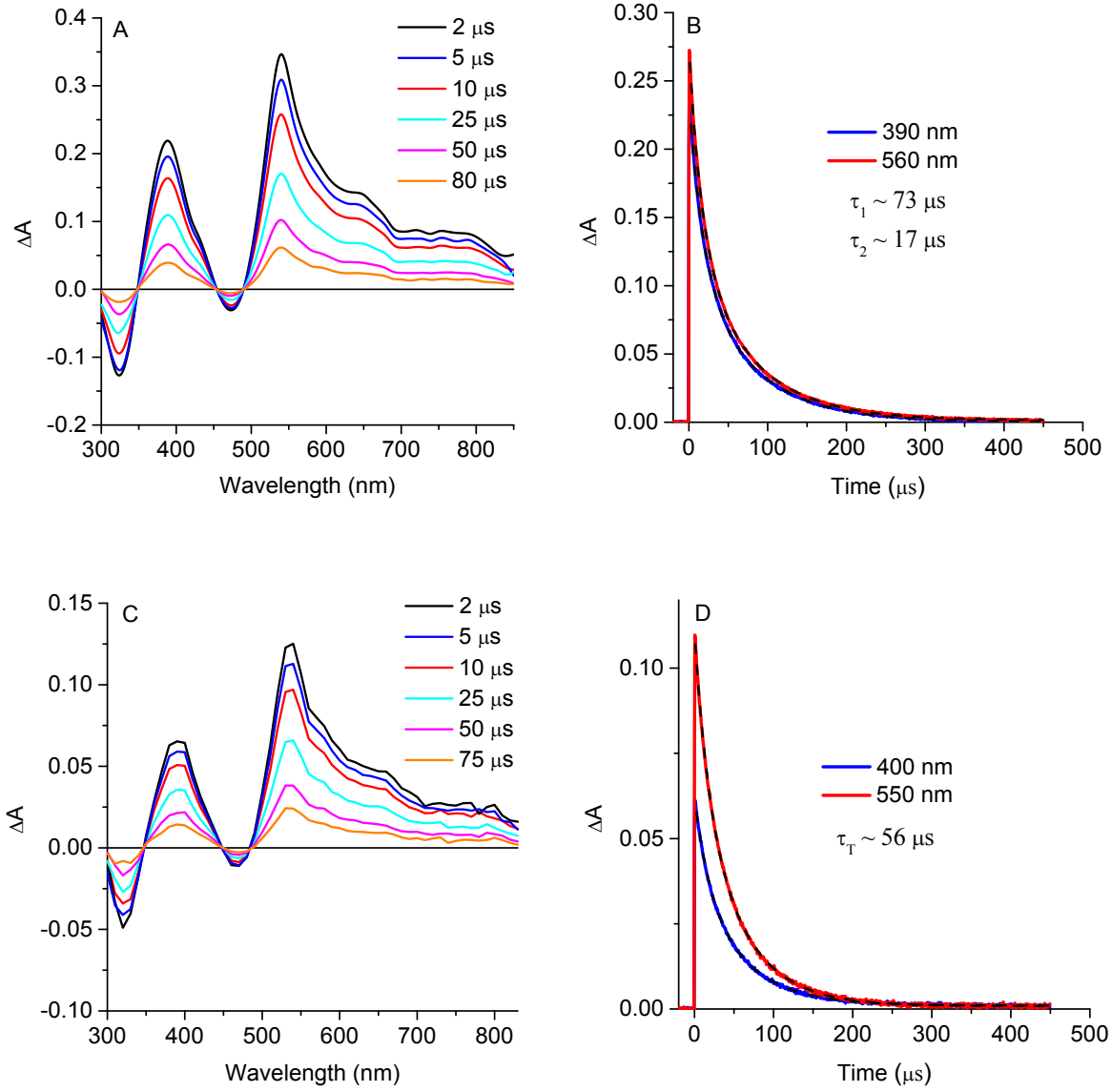

Figure 3. Transient absorption spectrum of **DPP-C_{60}** in (A) toluene and (C) DMF determined at different times after laser flash excitation at 532 nm in argon-saturated solution. (B) Absorption

View Article Online
DOI: 10.1039/C9OB02487E

decay monitored at 390 nm and 560 nm in toluene and (D) absorption decay monitored at 400 nm and 550 nm in DMF. Exponential adjustment of the triplet decay profiles (solid line).

Structure **C_{60}-DPP-C_{60}** showed a similar behavior in toluene (Figure 4A), with the main bands corresponding to the ^{3}DPP* (Figure S3A). As observed for **DPP-C_{60}**, the intensity of triplet absorbance was 20 times higher than that corresponding to the absorption of **DPP5**. In addition, it also showed two triplet-state lifetimes with magnitudes similar to those observed for **DPP-C_{60}**. On the other hand, the spectra presented a greater absorption in the region centered at 700 nm corresponding to the triplet of C_{60}. In DMF it can be observed that the intensity of this band is similar to that of ^{3}DPP* (Figure 4C). These results indicate that the structure formed by two C_{60} units efficiently populates the $^3C_{60}^*$, mainly in DMF.

Therefore, the transient absorption spectra indicate that linking covalently the DPP and C_{60} units creates structures with a high capacity to generate excited triplet states, when the DPP antenna is excited with green light. Furthermore, it was observed that the excited triplet state of the DPP antenna (^{3}DPP*) was mainly populated. ^{3}DPP* can be populated by a charge recombination process or by an EnT mechanism in which initially the energy is transferred from the excited singlet state of DPP (^{1}DPP*) to the $^1C_{60}$* unit, followed by ISC, and finalized by back-transfer of the triplet excitation from the $^3C_{60}$* to the ^{3}DPP*. Previously, Janssen and co-workers observed that a charge recombination process populates the ^{3}DPP* in hybrid structures based on a unit of thiophene-DPP directly linked to two C_{60} units.[78] In addition, the same authors studied similar structures but with alkyl linkers of different lengths between DPP and C_{60}, and found that the ^{3}DPP* is mainly populated by a back-transfer process from $^3C_{60}$*.[79] This last mechanism could be the predominant in the formation of triplet in **C_{60}-DPP-C_{60}**, considering the observed photophysical properties. In this regard, it was observed that the fluorescence in DMF was less quenched than in toluene (Figure 2). If a preponderant PeT process would be present, the fluorescence extinction would be higher in DMF since the charge-separated state is lower in energy in a solvent of higher polarity. Moreover,

an intense signal corresponding to $^3C_{60}$* is observed in the triplet spectra. In the case of **DPP-C$_{60}$**, triplet generation may be more favored by a charge recombination process, which leads to the formation of ^{3}DPP*. However, a competition between the two photophysical mechanisms cannot be ruled out for both conjugates.

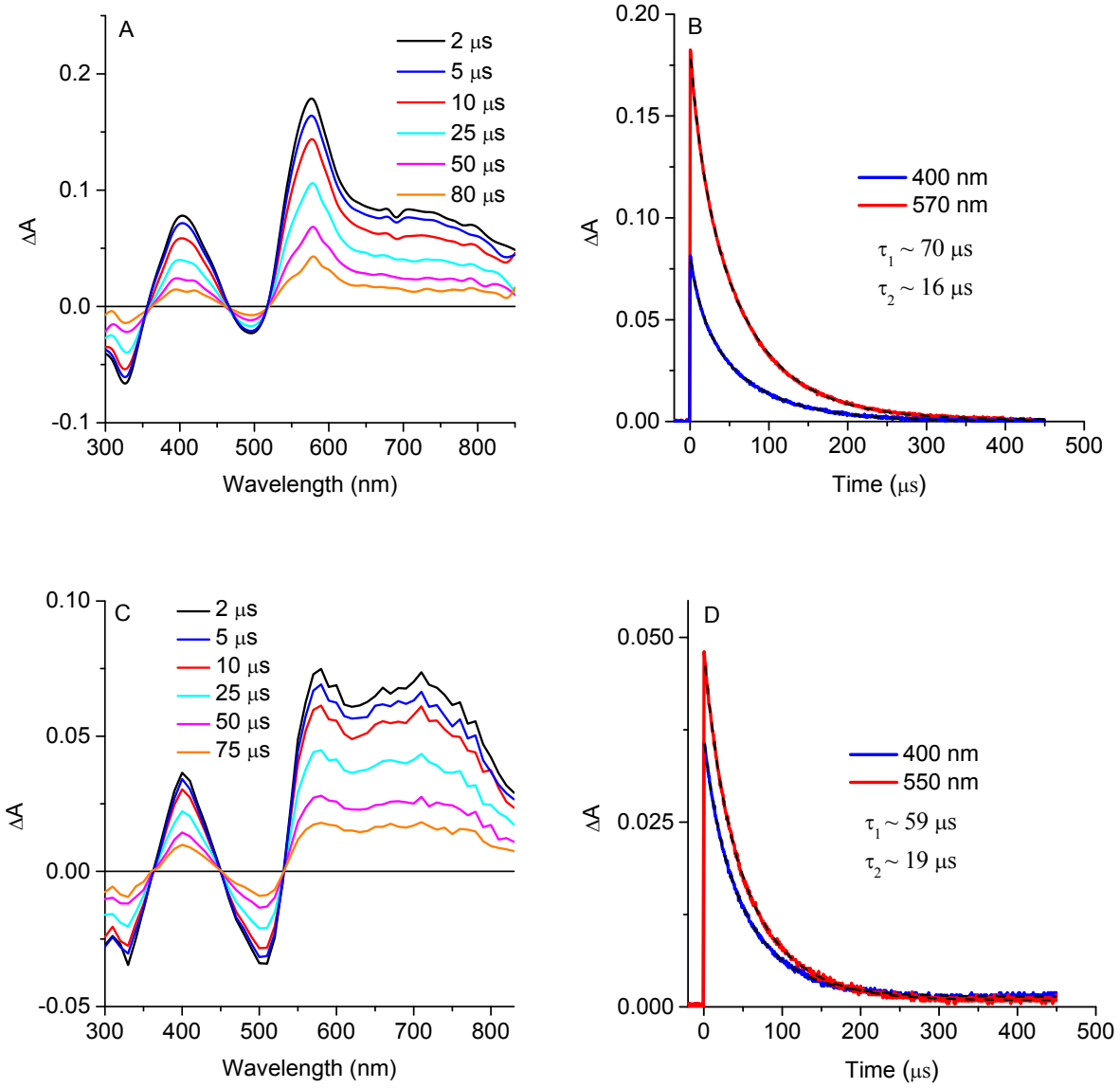

Figure 4. Transient absorption spectrum of **C$_{60}$-DPP-C$_{60}$** in (A) toluene and (C) DMF determined at different times after laser flash excitation at 532 nm in argon-saturated solution. (B) Absorption decay monitored at 400 nm and 570 nm in toluene and (D) absorption decay monitored at 400 nm and 550 nm in DMF. Exponential adjustment of the triplet decay profiles (solid line).

View Article Online
DOI: 10.1039/C9OB02487E

$O_2(^1\Delta_g)$ production

The $O_2(^1\Delta_g)$ production is a very important parameter to characterize the PSs efficiency for phototherapies, since a suitable production allows obtaining a greater photooxidation of the target cells. Here, the ability of the conjugates to produce $O_2(^1\Delta_g)$ was evaluated by the photodecomposition of DMA under aerobic conditions in toluene and DMF. DMA is a substrate that quenches $O_2(^1\Delta_g)$ by chemical reaction.[85] For comparative purposes, DMA reaction mediated by the DPP alone was also evaluated under the same experimental conditions. The samples were irradiated at 515 nm, therefore, the photophysical processes in **DPP-C_{60}** and **C_{60}-DPP-C_{60}** were initiated from the DPPs antennas. A time-dependent decrease in the DMA concentration was observed by following its absorbance at 378 nm (Figure S5). From first-order kinetic plots the values of the observed rate constant (k_{obs}) were calculated for DMA (Figure 5). Moreover, the values of Φ_Δ were determined comparing the slope for each compound with the slope obtained for the reference (**TMP**). The results obtained are compiled in Table 2.

In toluene, both conjugates showed great efficiency in the photodecomposition of DMA with slightly higher rates than a conventional PS as **TMP** (Figure 5A). **DPP-C_{60}** exhibited a Φ_Δ close to the unit (0.91), which is a little higher than that presented by **C_{60}-DPP-C_{60}** (0.75). These results are consistent with those observed in the transient spectra recorded in toluene, where **DPP-C_{60}** showed a higher generation of triplet states than **C_{60}-DPP-C_{60}**. After irradiation, the absorption due to these conjugates was unchanged indicating that they have a suitable photostability under the experimental conditions. On the other hand, the DPP derivatives without C_{60} showed very low $O_2(^1\Delta_g)$ generation efficiency capacities, in accordance with their photophysical properties previously observed (Figure 5A). Thus, if the Φ_Δ values of the **DPP-C_{60}** and **C_{60}-DPP-C_{60}** are compared with those corresponding to **DPP4** and **DPP5**, it is observed that **DPP-C_{60}** exhibited an efficiency 6-fold greater than **DPP4**, and **C_{60}-DPP-C_{60}** 12-fold higher than **DPP5**. In DMF, conjugates also presented an efficient production of $O_2(^1\Delta_g)$ with lower yields than in toluene

View Article Online
DOI: 10.1039/C9OB02487E

(Figure 5B). This behavior agrees with the lower population of triplet states observed in DMF (Figure 3C and 4C).

The efficiency obtained for both conjugates can be compared favorably with DPP derivatives evaluated as $O_2(^1\Delta_g)$ producers in similar experimental conditions. In this sense, Dong and co-workers designed an important number of DPP-based PSs. They reported a furan-DPP and thiophene-DPP-hyaluronic acid that showed $\Phi_\Delta \sim 0.40$ and 0.13 in DMF, respectively.[74,76] In addition, another structure based on thieno-indole-DPP exhibited an efficiency of 0.48 in CH_2Cl_2.[72] On the other hand, Ventura and collaborators reported the synthesis of two DPP-porphyrin systems which presented Φ_Δ around 0.50 in CH_2Cl_2.[86]

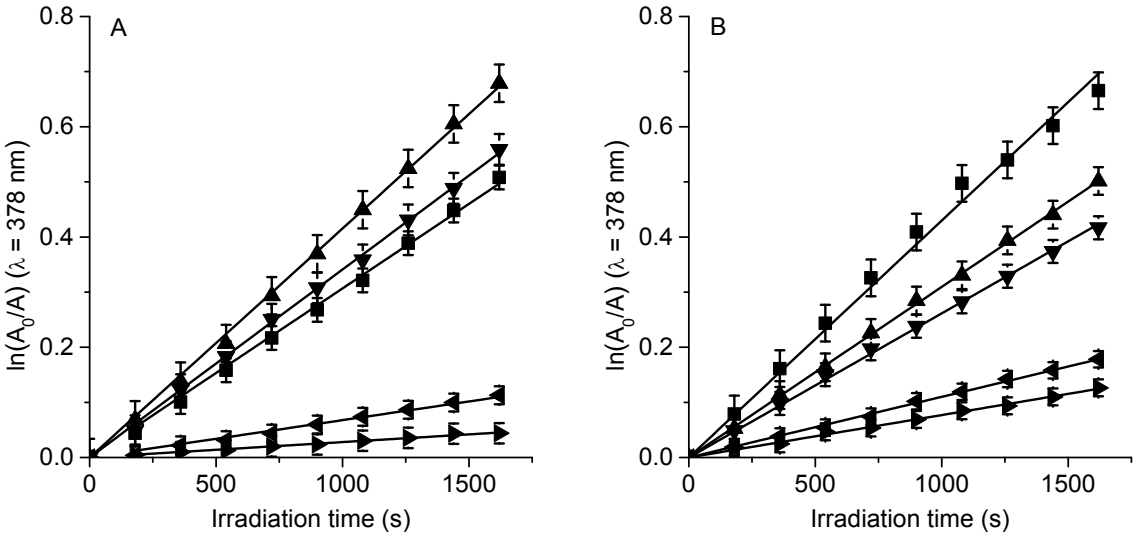

Figure 5. First-order plots for the photooxidation of DMA photosensitized by **DPP-C_{60}** (▲), **C_{60}-DPP-C_{60}** (▼), **DPP4** (◀), **DPP5** (▶) and **TMP** (■) in (A) toluene and (B) DMF; λ_{irr} = 515 nm.

Table 2. Kinetic parameters for the photooxidation of DMA (k_{obs}^{DMA}) and $O_2(^1\Delta_g)$ quantum yield (Φ_Δ).

Parameters	Media	**DPP4**	**DPP5**	**DPP-C_{60}**	**C_{60}-DPP-C_{60}**

View Article Online
DOI: 10.1039/C9OB02487E

k_{obs}^{DMA} (s^{-1})	toluene	(6.78±0.01)x10^{-5}	(2.79±0.05)x10^{-5}	(4.15±0.03)x10^{-4}	(3.41±0.02)x10^{-4}
Φ_Δ	toluene	0.15±0.01	0.06±0.01	0.91±0.03	0.75±0.02
k_{obs}^{DMA} (s^{-1})	DMF	(4.63±0.04)x10^{-5}	(7.69±0.09)x10^{-5}	(3.09±0.05)x10^{-4}	(2.61±0.04)x10^{-4}
Φ_Δ	DMF	0.07±0.01	0.11±0.01	0.47±0.02	0.39±0.02

Φ_Δ were calculated with TMP as reference: $k_{obs}^{toluene}$ = (3.07±0.03)x10^{-4} s^{-1} (Φ_Δ= 0.67) and k_{obs}^{DMF} = (4.30±0.06)x10^{-4} s^{-1} (Φ_Δ = 0.65).

To evaluate the antenna effect produced by the presence of DPP moieties, the photodecomposition of DMA sensitized by **DPP-C_{60}**, **C_{60}-DPP-C_{60}** and **MC_{60}** (Scheme S1), was compared using equal concentrations of each compound (5 μM). This assay was performed in toluene and the samples were irradiated with both monochromatic green light (515 nm) (Figure 6A) and white light (350-800 nm) (Figure 6B). When irradiated at 515 nm, k_{obs}^{DMA} = (2.51±0.04)x10^{-4} s^{-1} and (2.10±0.04)x10^{-4} s^{-1} were obtained for **DPP-C_{60}** and **C_{60}-DPP-C_{60}**, respectively. In addition, the DMA reaction photosensitized by **MC_{60}** yielded a k_{obs}^{DMA} = (6.99±0.02)x10^{-5} s^{-1}. The observed lower photodecomposition of DMA sensitized by **MC_{60}** was due to its very poor absorption in the green region of the spectrum. In this way, the presence of the visible light-harvesting DPP unit allows to enhance the efficiency by a factor of three when compared with that of the **MC_{60}**. On the other hand, when irradiated with visible light, higher rates of photooxidation were also observed for both conjugates (Figure 6B).

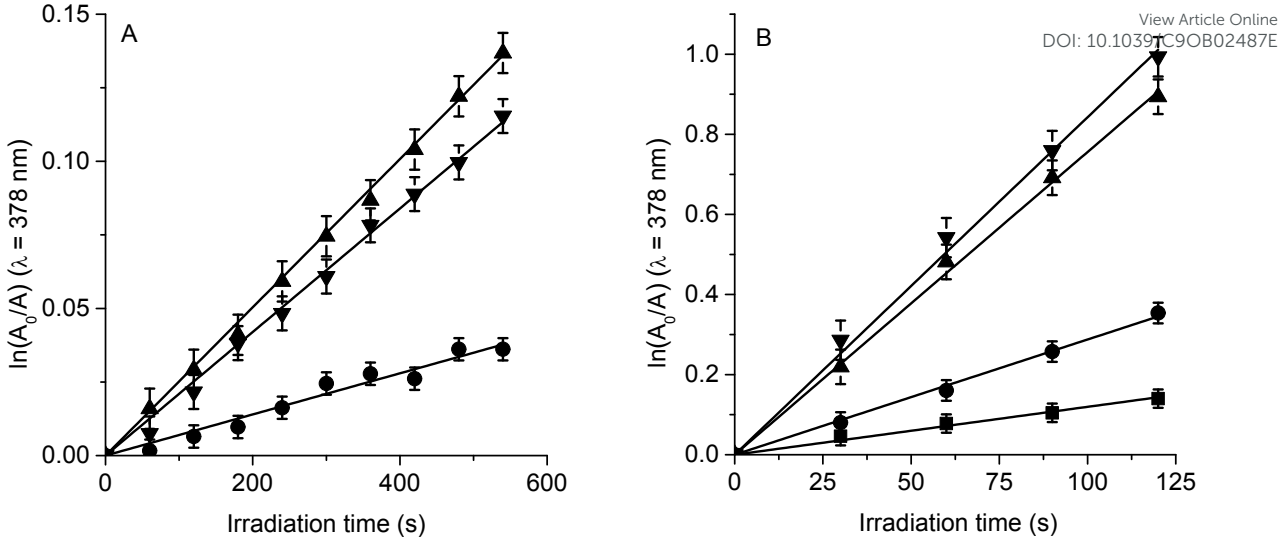

Figure 6. (A) First-order plots for the photooxidation of DMA photosensitized by **DPP-C_{60}** (▲), **C_{60}-DPP-C_{60}** (▼) and **MC_{60}** (●) at 5 μM PS in toluene; λ_{irr} = 515 nm. (B) Decreased absorption of DMA at 378 nm in presence of **DPP-C_{60}** (▲), **C_{60}-DPP-C_{60}** (▼) and **MC_{60}** (●) at 5 μM PS and DMA control (■) in toluene irradiated with visible light.

Photodynamic action in *S. aureus*

To observe if the antenna effect exerted by the DPP unit is still possible in a biological environment, photoinactivation of bacterial cultures sensitized by **DPP-C_{60}** and **C_{60}-DPP-C_{60}** was determined in *S. aureus* cell suspensions. For comparison, the photoinactivation mediated by **MC_{60}**, **DPP4** and **DPP5** was also examined. The cultures were treatment with 10 μM PS and irradiated with green LED light (510 nm). Microbial survivals are shown in Figure 7. Low toxicity was observed for the cells treated with 10 μM PS in the dark (Figure 7, lines 2, 3, 4, 5 and 6 for **DPP4**, **DPP5**, **DPP-C_{60}** and **C_{60}-DPP-C_{60}**, respectively). After 15 min irradiation, **DPP-C_{60}** and **C_{60}-DPP-C_{60}** induced a similar reduction of ~3 log in the cell survival of *S. aureus* (Figure 7, lines 10 and 11), while **DPP4** and **DPP5** caused an inactivation of ~1 log (Figure 7, lines 8 and 9). Also, negligible photokilling was observed using **MC_{60}**. The limited photoinactivation activity found with DPP structures agrees with the low capacity of these compounds to form excited triplet state and

View Article Online
DOI: 10.1039/C9OB02487E

consequently the low production of ROS. In contrast, the insignificant effect of **MC_{60}** can be mainly associated with the very low absorption of visible light in the central area of the spectrum by the fullerene C_{60} derivatives.[33,86] However, these biological essays indicate that the conjugates have photocytotoxic activity in *S. aureus*. The photodynamic activity mediated by **DPP-C_{60}** and **C_{60}-DPP-C_{60}** represents a value greater than 99.9% of cell inactivation. However, the efficiency found *in vitro* does not agree with the excellent photophysical properties observed in solution for both conjugates. We believe that the high hydrophobic nature of the PSs decreases photodynamic activity in biological media. To solve this limitation, different strategies could be approached: 1) to prepare water-soluble nanoparticles of each PS for *in vitro* application using known methods [73,74,88]; 2) to incorporate cationic groups by methylation of tertiary amines.[33,34,86] Those cationic groups would not only grant a greater amphiphilic character to the structures, but also, the positive charge may allow to increase the interaction with the negatively charged biological membranes and thus optimize the photodynamic action;[59] 3) the chlorine atom present in **DPP-C_{60}** is a versatile site for further modifications that allow to attach neutral or ionic hydrophilic groups at the DPP core.[70,71] Currently, investigations in some of these directions are being carried out in our labs to enhance the photodynamic capacity of the DPP–fullerene conjugates in biologic media.

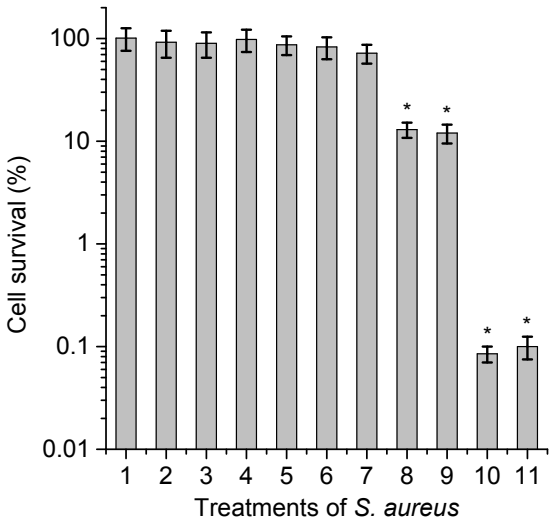

Figure 7. Survival of *S. aureus* (~10^8 CFU/mL) treated with 10 μM PS for 15 min in the dark and

View Article Online
DOI: 10.1039/C9OB02487E

irradiated with green light for 15 min; 1) cells without PS in the dark, 2) cells treated with **MC_{60}** in the dark, 3) cells treated with **DPP4** in the dark, 4) cells treated with **DPP5** in the dark, 5) cells treated with **DPP-C_{60}** in the dark, 6) cells treated with **C_{60}-DPP-C_{60}** in the dark, 7) irradiated cells treated with **MC_{60}**, 8) irradiated cells treated with **DPP4**, 9) irradiated cells treated with **DPP5**, 10) irradiated cells treated with **DPP-C_{60}** and 11) irradiated cells treated with **C_{60}-DPP-C_{60}** (*$p<0.05$, compared with control).

Conclusions

In this work, we presented the preparation of two conjugates formed by visible light-harvesting antennas of DPPs derivatives (intramolecular energy/electron donor) and C_{60} fullerene (intramolecular energy/electron acceptor and ISC converter). These structures presented high capacity to produce excited triplet states when DPPs antennas were photoexcited. The efficiency in triplet production of conjugates **DPP-C_{60}** and **C_{60}-DPP-C_{60}** is 20 times higher than that corresponding to the DPPs alone. Excited triplet states can be populated by a process of charge recombination or back-transfer of the triplet excitation. Moreover, both conjugates exhibited very high efficiency in $O_2(^1\Delta_g)$ generation, with yields close to unity in toluene and around 0.5 in a more polar medium, such as DMF. In addition, **DPP-C_{60}** and **C_{60}-DPP-C_{60}** architectures showed greater $O_2(^1\Delta_g)$ production that those sensitized by DPPs and C_{60} moieties. Thus, we demonstrated for the first time that the covalent linked between C_{60} and DPPs allows generating hybrid PSs with high ability to produce $O_2(^1\Delta_g)$. On the other hand, studies *in vitro* of PDI indicated that these conjugates present photocytotoxic effect in *S. aureus* cell suspensions. Further strategies must be carried out in order to increase the biocompatibility of the PSs and consequently their photodynamic efficiencies in biological media. In summary, results revealed that DPP-C_{60} structures offer a promising molecular architecture to act as potential heavy atom-free PSs in photodynamic inactivation and other applications where $O_2(^1\Delta_g)$ is required.

View Article Online
DOI: 10.1039/C9QB02487E

Acknowledgements

Authors are grateful to Consejo Nacional de Investigaciones Científicas y Técnicas (CONICET, Argentina), Universidad Nacional de Río Cuarto (UNRC, Argentina) and Universidade de Aveiro (Portugal). The authors are grateful to CONICET (PIP-2015 1122015 0100197 CO), UNRC (PPI-2016 18/C460), ANPCYT (PICT 0667/16) and MINCyT Córdoba PID Nº 000144/18, 000007/19 for financial support. N.S.G. and E.N.D. are Scientific Members of CONICET. M.L.A. thanks CONICET for the research fellowship. Thanks are also due to Fundacão para a Ciência e a Tecnologia (Portugal) for the financial support to project PTDC/QEQ-QOR/6160/2014 and to the research unit UID/QUI/00062/2019. The collaboration between the two scientific groups was possible thanks to a research grant awarded by the Asociación Universitaria Iberoamericana de Postgrado (AUIP, Salamanca, Spain) to M.L.A.

References

1 J. Zhao, W. Wu, J. Sun and S. Guo, *Chem. Soc. Rev.*, 2013, **42**, 5323–5351.

2 C. K. Prier, D. A. Rankic and D. W. C. MacMillan, *Chem. Rev.*, 2013, **113**, 5322–5363.

3 Y.-Q. Zou, J.-R. Chen, X.-P. Liu, L.-Q. Lu, R. L. Davis, K. A. Jørgensen and W.-J. Xiao, *Angew. Chemie Int. Ed.*, 2012, **51**, 784–788.

4 F. Guo, Y.-G. Kim, J. R. Reynolds and K. S. Schanze, *Chem. Commun.*, 2006, 1887–1889.

5 F. Etzold, I. A. Howard, N. Forler, A. Melnyk, D. Andrienko, M. R. Hansen and F. Laquai, *Energy Environ. Sci.*, 2015, **8**, 1511–1522.

6 T. N. Singh-Rachford and F. N. Castellano, *Coord. Chem. Rev.*, 2010, **254**, 2560–2573.

7 J. Zhou, Q. Liu, W. Feng, Y. Sun and F. Li, *Chem. Rev.*, 2015, **115**, 395–465.

8 Y. Cakmak, S. Kolemen, S. Duman, Y. Dede, Y. Dolen, B. Kilic, Z. Kostereli, L. T. Yildirim, A. L. Dogan, D. Guc and E. U. Akkaya, *Angew. Chemie Int. Ed.*, 2011, **50**, 11937–11941.

9 A. Kamkaew, S. H. Lim, H. B. Lee, L. V. Kiew, L. Y. Chung and K. Burgess, *Chem. Soc. Rev.*, 2013, **42**, 77–88.

View Article Online
DOI: 10.1039/C9OB02487E

10 M. R. Hamblin, *Curr. Opin. Microbiol.*, 2016, **33**, 67–73.

11 H. Abrahamse and M. R. Hamblin, *Biochem. J.*, 2016, **473**, 347–364.

12 A. Tavares, C. M. B. Carvalho, M. A. Faustino and M. G. P. M. S. Neves, *Mar Drugs*, 2010, **8**, 91–105.

13 D. D. Ferreyra, M. B. Spesia, M. E. Milanesio and E. N. Durantini, *J. Photochem. Photobiol. A Chem.*, 2014, **282**, 16–24.

14 E. N. Durantini, *Curr. Bioact. Compd.*, 2006, **2**, 127–142.

15 P. R. Ogilby, *Photochem. Photobiol. Sci.*, 2010, **9**, 1543.

16 T. G. St. Denis, T. Dai, L. Izikson, C. Astrakas, R. R. Anderson, M. R. Hamblin and G. P. Tegos, *Virulence*, 2011, **2**, 509–520.

17 D. A. Phoenix, Z. Sayed, S. Hussain, F. Harris and M. Wainwright, *FEMS Immunol. Med. Microbiol.*, 2003, **39**, 17–22.

18 M. Tim, *J. Photochem. Photobiol. B Biol.*, 2015, **150**, 2–10.

19 M. G. Alvarez, M. N. Montes, D. Oca, M. E. Milanesio, C. S. Ortiz and E. N. Durantini, *Photodiagnosis Photodyn. Ther.*, 2014, **11**, 148–155.

20 C. Simões, M. C. Gomes, M. G. P. M. S. Neves, Â. Cunha, J. P. C. Tomé, A. C. Tomé, J. A. S. Cavaleiro, A. Almeida and M. A. F. Faustino, *Catal. Today*, 2016, **266**, 197–204.

21 S. J. Mora, M. P. Cormick, M. E. Milanesio and E. N. Durantini, *Dye. Pigment.*, 2010, **87**, 234–240.

22 Y. Arenas, S. Monro, G. Shi, A. Mandel, S. Mcfarland and L. Lilge, *Photodiagnosis Photodyn. Ther.*, 2013, **10**, 615–625.

23 S. Jianzhang, *J. Mater. Chem. B*, 2014, **2**, 2838–2854.

24 E. Karakus, E. K. Demirci, M. Sayar and S. Dartar, *Org. Lett.*, 2017, **19**, 2522–2525.

25 T. Yogo, Y. Urano, Y. Ishitsuka, F. Maniwa and T. Nagano, *J. Am. Chem. Soc.*, 2005, **127**, 12162–12163.

26 A. C. B. P. Costa, V. M. C. Rasteiro, C. A. Pereira, R. D. Rossoni, J. C. Junqueira and A. O.

C. Jorge, *Mycoses*, 2012, **55**, 56–63.

View Article Online
DOI: 10.1039/C9OB02487E

27 S. H. Lim, C. Thivierge, P. Nowak-Sliwinska, J. Han, H. van den Bergh, G. Wagnières, K. Burgess and H. B. Lee, *J. Med. Chem.*, 2010, **53**, 2865–2874.

28 M. Laine, N. A. Barbosa, A. Kochel, B. Osiecka, G. Szewczyk, T. Sarna, P. Ziółkowski, R. Wieczorek and A. Filarowski, *Sens Actuators B Chem*, 2017, **238**, 548–555.

29 J. Zhao, K. Chen, Y. Hou, Y. Che, L. Liu and D. Jia, *Org. Biomol. Chem.*, 2018, **16**, 3692–3701.

30 Y. Wei, M. Zheng, Q. Zhou, X. Zhou and S. Liu, *Org. Biomol. Chem.*, 2018, **16**, 5598–5608.

31 J. Zhao, K. Xu, W. Yang, Z. Wang and F. Zhong, *Chem. Soc. Rev.*, 2015, **44**, 8904–8939.

32 D. M. Guldi and M. Prato, *Acc. Chem. Res.*, 2000, **33**, 695–703.

33 S. K. Sharma, L. Y. Chiang and M. R. Hamblin, *Nanomedicine*, 2011, **6**, 1813–1825.

34 M. L. Agazzi, M. B. Spesia, N. S. Gsponer, M. E. Milanesio and E. N. Durantini, *J. Photochem. Photobiol. A Chem.*, 2015, **310**, 171–179.

35 N. S. Gsponer, M. L. Agazzi, M. B. Spesia and E. N. Durantini, *Methods*, 2016, **109**, 167–174.

36 M. B. Spesia, M. E. Milanesio and E. N. Durantini, in *Nanostructures for Antimicrobial Therapy*, Elsevier, 2017, pp. 413–433.

37 D. M. Guldi and K. D. Asmus, *J. Phys. Chem. A*, 1997, **101**, 1472–1481.

38 W. Wu, J. Zhao, J. Sun and S. Guo, *J. Org. Chem.*, 2012, **77**, 5305–5312.

39 P. Yang, W. Wu, J. Zhao, D. Huang and X. Yi, *J. Mater. Chem.*, 2012, **22**, 20273.

40 Y. Wei, M. Zhou, Q. Zhou, X. Zhou, S. Liu, S. Zhang and B. Zhang, *Phys. Chem. Chem. Phys.*, 2017, **19**, 22049–22060.

41 D. M. Guldi, M. Maggini, G. Scorrano and M. Prato, *J. Am. Chem. Soc.*, 1997, **119**, 974–980.

42 R. Koeppe and N. S. Sariciftci, *Photochem. Photobiol. Sci.*, 2006, **5**, 1122–1131.

43 R. Ziessel, B. D. Allen, D. B. Rewinska and A. Harriman, *Chem. - A Eur. J.*, 2009, **15**, 7382–7393.

44 C. C. Hofmann, S. M. Lindner, M. Ruppert, A. Hirsch, S. A. Haque, M. Thelakkat and J. Köhler, *J. Phys. Chem. B*, 2010, **114**, 9148–9156.

45 W.-J. Shi, M. E. El-Khouly, K. Ohkubo, S. Fukuzumi and D. K. P. Ng, *Chem. Eur. J.*, 2013, **19**, 11332–11341.

46 V. Bandi, S. K. Das, S. G. Awuah, Y. You and F. D'Souza, *J. Am. Chem. Soc.*, 2014, **136**, 7571–7574.

47 J.-Y. Liu, M. E. El-Khouly, S. Fukuzumi and D. K. P. Ng, *Chem. - An Asian J.*, 2011, **6**, 174–179.

48 V. Bandi, H. B. Gobeze, V. Lakshmi, M. Ravikanth and F. D'Souza, *J. Phys. Chem. C*, 2015, **119**, 8095–8102.

49 C. O. Obondi, G. N. Lim, P. A. Karr, V. N. Nesterov and F. D'Souza, *Phys. Chem. Chem. Phys.*, 2016, **18**, 18187–18200.

50 L. Huang, X. Yu, W. Wu and J. Zhao, *Org. Lett.*, 2012, **14**, 2594–2597.

51 L. Huang, X. Cui, B. Therrien and J. Zhao, *Chem. - A Eur. J.*, 2013, **19**, 17472–17482.

52 L. Huang and J. Zhao, *Chem. Commun.*, 2013, **49**, 3751–3753.

53 L. Huang and J. Zhao, *J. Mater. Chem. C*, 2015, **3**, 538–550.

54 H. Ünlü and E. Okutan, *Dye. Pigment.*, 2017, **142**, 340–349.

55 M. L. Agazzi, J. E. Durantini, N. S. Gsponer, A. M. Durantini, S. G. Bertolotti and E. N. Durantini, *ChemPhysChem*, 2019, **20**, 1110–1125.

56 M. Milanesio, M. Alvarez, V. Rivarola, J. Silber and E. Durantini, *Photochem. Photobiol.*, 2005, **81**, 891–897.

57 M. G. Alvarez, C. Prucca, M. E. Milanesio, E. N. Durantini and V. Rivarola, *Int. J. Biochem. Cell Biol.*, 2006, **38**, 2092–2101.

58 C. Constantin, M. Neagu, R.-M. Ion, M. Gherghiceanu and C. Stavaru, *Nanomedicine*, 2010,

5, 307–317.

View Article Online
DOI: 10.1039/C9OB02487E

59 M. B. Ballatore, M. B. Spesia, M. E. Milanesio and E. N. Durantini, *Eur. J. Med. Chem.*, 2014, **83**, 685–694.

60 L. Y. Chiang, P. A. Padmawar, J. E. Rogers-Haley, G. So, T. Canteenwala, S. Thota, L.-S. Tan, K. Pritzker, Y.-Y. Huang, S. K. Sharma, D. B. Kurup, M. R. Hamblin, B. Wilson and A. Urbas, *J. Mater. Chem.*, 2010, **20**, 5280–5293.

61 R. Yin, M. Wang and Y. Huang, *Nanomedicine Nanotechnology, Biol. Med.*, 2014, **10**, 795–808.

62 R. Yin, M. Wang, Y. Huang, G. Landi, D. Vecchio, L. Y. Chiang and M. R. Hamblin, *Free Radic. Biol. Med.*, 2015, **79**, 14–27.

63 S.-E. Zhu, K.-Q. Liu, X.-F. Wang, A.-D. Xia and G.-W. Wang, *J. Org. Chem.*, 2016, **81**, 12223–12231.

64 Y. Liu and J. Zhao, *Chem. Commun.*, 2012, **48**, 3751–3753.

65 S. Guo, J. Sun, L. Ma, W. You, P. Yang and J. Zhao, *Dye. Pigment.*, 2013, **96**, 449–458.

66 A. Y. Rybkin, A. Y. Belik, O. A. Kraevaya, E. A. Khakina, A. V Zhilenkov, N. S. Goryachev, D. Volyniuk, J. V Grazulevicius, P. A. Troshin and A. I. Kotelnikov, *Dye. Pigment.*, 2019, **160**, 457–466.

67 F. Wang, X. Cui, Z. Lou, J. Zhao, M. Bao and X. Li, *Chem. Commun.*, 2014, **50**, 15627–15630.

68 Q. Tang, W. Xiao, J. Li, D. Chen, Y. Zhang, J. Shao and X. Dong, *J. Mater. Chem. B*, 2018, **6**, 2778–2784.

69 M. Grzybowski and D. T. Gryko, *Adv. Opt. Mater.*, 2015, **3**, 280–320.

70 M. Kaur and D. H. Choi, *Chem. Soc. Rev.*, 2015, **44**, 58–77.

71 S. Luňák, M. Vala, J. Vyňuchal, I. Ouzzane, P. Horáková, P. Možíšková, Z. Eliáš and M. Weiter, *Dye. Pigment.*, 2011, **91**, 269–278.

72 J. Yang, Y. Cai, Y. Zhou, C. Zhang, P. Liang, B. Zhao, J. Shao, N. Fu, W. Huang and X.

Dong, *Dye. Pigment.*, 2017, **147**, 270–282.

View Article Online
DOI: 10.1039/C9OB02487E

73 Y. Cai, P. Liang, W. Si, B. Zhao, J. Shao, W. Huang, Y. Zhang, Q. Zhang and X. Dong, *Org. Chem. Front.*, 2018, **5**, 98–105.

74 P. Liang, Y. Wang, P. Wang, J. Zou, H. Xu, Y. Zhang, W. Si and X. Dong, *Nanoscale*, 2017, **9**, 18890–18896.

75 H. Shi, W. Sun, Q. Wang, G. Gu, W. Si, W. Huang, Q. Zhang and X. Dong, *ChemPlusChem*, 2016, **81**, 515–520.

76 Y. Cai, Q. Tang, X. Wu, W. Si, W. Huang, Q. Zhang and X. Dong, *ChemistrySelect*, 2016, **1**, 3071–3074.

77 Y. Cai, Q. Tang, X. Wu, W. Si, Q. Zhang, W. Huang and X. Dong, *ACS Appl. Mater. Interfaces*, 2016, **8**, 10737–10742.

78 B. P. Karsten, R. K. M. Bouwer, J. C. Hummelen, R. M. Williams and R. A. J. Janssen, *Photochem. Photobiol. Sci.*, 2010, **9**, 1055–1065.

79 B. P. Karsten, P. P. Smith, A. B. Tamayo and R. A. J. Janssen, *J. Phys. Chem. A*, 2012, **116**, 1146–1150.

80 J. Wang, Y. Hou, W. Lei, Q. Zhou, C. Li, B. Zhang and X. Wang, *ChemPhysChem*, 2012, **13**, 2739–2747.

81 M. Maggini, G. Scorrano and M. Prato, *J. Am. Chem. Soc.*, 1993, **115**, 9798–9799.

82 E. Reynoso, E. D. Quiroga, M. L. Agazzi, M. B. Ballatore, S. G. Bertolotti and E. N. Durantini, *Photochem. Photobiol. Sci.*, 2017, **16**, 1524–1536.

83 M. E. Milanesio, M. G. Alvarez, E. I. Yslas, C. D. Borsarelli, J. J. Silber, V. Rivarola and E. N. Durantini, *Photochem. Photobiol.*, 2007, **74**, 14–21.

84 M. Prato and M. Maggini, *Acc. Chem. Res.*, 1998, **31**, 519–526.

85 A. Gomes, E. Fernandes and J. L. F. C. Lima, *J. Biochem. Biophys. Methods*, 2005, **65**, 45–80.

86 J. Schmitt, V. Heitz, A. Sour, F. Bolze, H. Ftouni, J. F. Nicoud, L. Flamigni and B. Ventura,

Angew. Chemie - Int. Ed., 2015, **54**, 169–173.

View Article Online
DOI: 10.1039/C9OB02487E

87 M. B. Spesia, M. E. Milanesio and E. N. Durantini, *Eur. J. Med. Chem.*, 2008, **43**, 853–861.

88 Y. Cai, P. Liang, Q. Tang, W. Si, P. Chen, Q. Zhang and X. Dong, *ACS Appl. Mater. Interfaces*, 2017, **9**, 30398–30405.